

PHASE-FIELD SOLUTIONS FOR THE CLASSIC ONE-DIMENSIONAL TWO-PHASE SUPERCOOLED SOLIDIFICATION PROBLEM

Maurício Fabbri¹

KEYWORDS: Solidification, Phase-Field Methods, Stefan Problems.

ABSTRACT: Results for the two-phase supercooled Stefan problem on a finite domain are obtained by a numerical Phase-Field (PF) model. The PF results are shown to be made as close as desired to the classical sharp-interface similarity solution, in the semi-infinite domain limit. A basic engineering introduction to PF modeling and guidelines for a simple fixed-grid computational implementation are also given.

INTRODUCTION

The numerical modeling of solidification processes has to deal with the location of the solid-liquid (SL) interface, which is not known in advance. The prototype of such “free-boundary” problems is the so-called Stefan solidification, which consists of a slab of a pure substance initially at a definite state (e.g., liquid), that undergoes phase-change as heat is exchanged with the surrounding medium across the wall at $x=0$ (see Fig. 1).

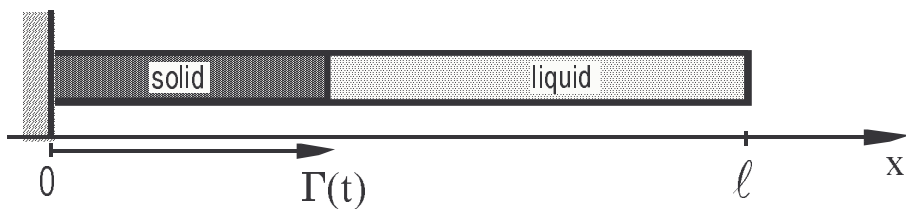


Fig. 1 – One-dimensional (Stefan) slab solidification. Analytical solutions are known for simple boundary and initial conditions and when the domain $[0, l]$ is semi-infinite ($l \rightarrow \infty$).

For semi-infinite domains, the Stefan solidification problem admits a solution within the similarity class x/\sqrt{t} ; as a consequence, the S-L interface progression is given by

¹ Prof. Dr., Faculdade de Engenharia – FE, Universidade São Francisco – USF
Rua Alexandre Rodrigues Barbosa, 45, 13251-900 Itatiba SP Brazil, e-mail fabbri@usf.br

$\Gamma(t) = b\sqrt{t}$, where the constant b is a root of a well-known transcendental equation (the Newman solution^{1,2}). There is no analytical solution for the finite slab solidification, and/or when the thermophysical properties of the medium are not constant; for those cases, semi-analytical or numerical methods are required.

There are two broad classes of traditional numerical approaches to deal with free-boundary problems, namely, (1) the front-tracking techniques, where the position of the interface is explicitly followed during the discrete time-integration, and (2) the so-called “enthalpy” technique and its variants, where the problem is re-formulated in terms of a global variable that does not explicitly depends on the local phase – like using the energy (or the enthalpy) instead of temperature as the main variable in solidification models. A third alternative - the Phase Field (PF) model - gained recognition during the last decade, which allows for a better physical formulation of the phase-change problem; it introduces an “order parameter” to indicate the phase state, working along the ideas of the phase transition theories far from the critical point.

The limitations of the traditional “enthalpy” techniques become apparent even in their simplest formulations. For a pure substance, with constant thermophysical properties, the enthalpy H as a function of temperature T can be simply defined as:

$$H = \begin{cases} c_s(T - T_m) & \text{for } T \leq T_m \text{ (solid state)} \\ c_l(T - T_m) + L & \text{for } T > T_m \text{ (liquid state)} \end{cases} \quad (\text{Eq. 1})$$

, where T_m is the melting temperature, L is the latent heat of fusion and $c_{s,l}$ are the specific heats of the solid and liquid phases, respectively. Now the enthalpy flux (for constant-volume systems, the difference between enthalpy and energy is immaterial) is determined from the temperature distribution via the Fourier law, so the traditional heat conduction equation can be written as

$$\frac{\partial H}{\partial t} = \nabla^2 T \quad (\text{Eq. 2})$$

Given a temperature distribution at time t , we can therefore update the enthalpy for time $t + \Delta t$ by Eq. 2, and then invert Eq. 1 to find the new temperature field. Note that Eq. 1, in fact, states that the phase state is a unique function of temperature, and that is precisely the weakness of the enthalpy model – since it is a common fact that materials can be supercooled

or superheated: experience shows that there can be a liquid phase for $T < T_m$ and (more rarely) solid for $T > T_m$.

It is to be noted that the same limitations do apply for the majority of the “front-tracking” techniques, since they assume an explicit relationship between the local temperature and the phase state.

To overcome that fundamental difficulty we must formulate the phase change as a dynamical process which depends on the local free-energy, which in turn is a function of temperature, in a manner that favors (but not determine) the liquid state for $T > T_m$. That is exactly the main idea of the Phase-Field (PF) model, which we now briefly describe.

THE PHASE-FIELD MODEL

Let a phase variable $p(x,t)$ be introduced, the values of which describe the phase state of the material. We choose the value +1 corresponding to liquid, and -1 to solid. The S-L interface is defined by points at which $p=0$. In practice, there is always a transition layer of width ε between the solid and liquid phases (Fig. 2), which can be made as small as desired, in order to approximate a sharp interface.

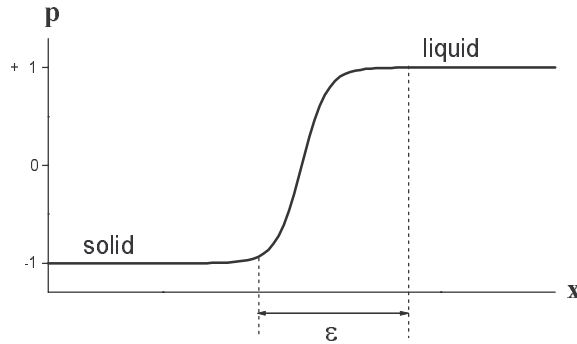


Fig. 2 – The order parameter in the PF model describes a diffuse interface between phases, with characteristic length ε

Caginalp & Sokolowsky³ and Fabbri & Voller⁴ have shown that the use of a suitable large numerical value for ε does not compromise the solutions of the PF equations (that does, however, introduce a cutoff for short wavelengths which could hinder a selection process in a non-isotropic multidimensional medium – a pertinent issue for the theory of dendrite fingering, for instance).

In equilibrium, the spatial profile of $p(x,t)$ minimizes the total free-energy F of the system (or any other thermodynamically consistent functional). In terms of a first-order expansion in the field p , and the temperature T , F is written as:

$$F = \int \left\{ \frac{1}{2} \xi^2 |\nabla p|^2 + F(p, T) \right\} d^3 r \quad (\text{Eq. 3})$$

, where $F(p, T)$ is a double-well potential having local minima at $p = \pm 1$, and ξ is a characteristic length of order ε .

Solidification (that is, the S-L interface progression) is driven by the potential term $F(p, T)$, which therefore should have the form depicted in Fig.3, exhibiting minima at $p = \pm 1$, corresponding to equilibrium solid and liquid states.

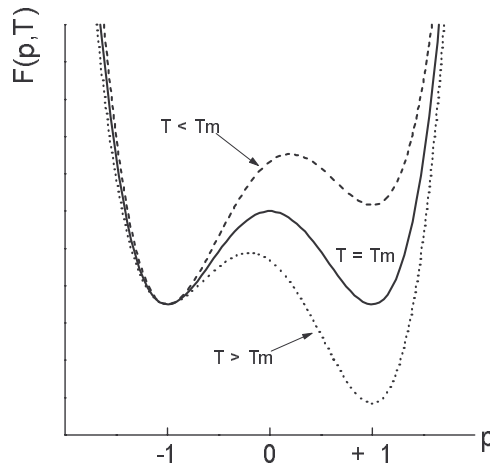


Fig. 3 – The phase-field potential, with temperature-dependent relative minima height positions. T_m is the melting temperature.

Minimization of the functional F (Eq.3) with respect to the order parameter p , followed by a relaxation-time approximation⁵ with characteristic time α , gives the evolution equation

$$\alpha \xi^2 \frac{\partial p}{\partial t} = \xi^2 \nabla^2 p - \frac{\partial F}{\partial p} \quad (\text{Eq.4})$$

Eq. 4 can be given the following physical interpretation⁵. The derivative $-\partial F / \partial p$ plays the role of a thermodynamic driving force for phase change, with respect to the coordinate p . At a temperature T equal to the equilibrium melting temperature T_m , the two minima at $p = \pm 1$ have exactly the same energy; for $T > T_m$, the minimum at $p = +1$ has lower energy (the liquid state is the stable state, the solid state being a possible metastable state above the equilibrium melting temperature), and conversely for $T < T_m$. The natural tendency of the system is to

relax towards equilibrium, with respect to spatial fluctuations in the phase value $p(x,t)$; this is in fact the origin of surface tension effects, and it is accounted for by the term $\xi^2 \nabla^2 p$. When the system is at equilibrium, every point of it is sitting in a minimum of $F(p,x)$, at $p=+1$ or -1 , except at some possible transition layers where the value of p undergoes steep changes; if those layers are not moving, then, locally, the driving force $-\partial F/\partial p$ balances exactly the surface tension term. In the event that the system is out of equilibrium, the time evolution of $p(x,t)$ is assumed to be proportional to the imbalance between the potential and the surface tension energy - this leads to a velocity-dependent term which includes, in a natural way, the kinetic relaxation during front progression.

The diffuse interface theory of Allen & Cahn⁶ relates the surface tension σ to the potential F and to the characteristic length ξ , as follows:

$$\sigma = \sqrt{2}\xi \int_{-1}^{+1} \sqrt{F(p,T)} dp \quad (\text{Eq. 5})$$

At this level of macroscopic modeling of solidification, the potential $F(p,T)$ can be chosen by numerical convenience, provided it has the qualitative features depicted in Fig.3. We follow Kobayashi⁷, and write $F(p,T)$ as a fourth degree polynomial with fixed minima at ± 1 :

$$F(p,T) = W \int_{-1}^{p} (1 - \phi^2)(\phi + m(T)) d\phi \quad (\text{Eq. 6})$$

W is an arbitrary constant (related to the entropy scale), and the temperature-dependent term $m(T)$ must satisfy $|m(T)| < 1$, in order to have dF/dp with three distinct roots. We choose a simple linear form (from here on, we assume $T_m=0$):

$$m(T) = \gamma T \quad (\text{Eq. 7})$$

, restricting γ to a maximum value such that $-1 < m < +1$ for every possible value of temperature the system may exhibit.

A quick asymptotic expansion of the solutions of Eq.4 around an interface then shows that the temperature at the interface is proportional to the front velocity $v=d\Gamma/dt$,

$$T(x = \Gamma) = - \left(\frac{3\sigma\alpha}{4\gamma W} \right) v \quad (\text{Eq. 8})$$

Eq.8 shows that the PF model incorporates automatically the kinetic effect at the SL front, and the temperature of a moving interface must be lower than the equilibrium

temperature T_m . Non-linear kinetic effects can also be accounted for¹⁰, and a non-linear relaxation-time model evolution is also possible⁸.

Eq.4 for the phase field must be coupled to a heat transport equation for temperature, which presently is simply the usual Fourier law with a source term to account for the latent heat release at the interface:

$$\rho c \frac{\partial T}{\partial t} + \frac{1}{2} \rho L \frac{\partial p}{\partial t} = K \nabla^2 T \quad (\text{Eq. 9})$$

ρ, K and c are the medium density, conductivity and specific heat, respectively. Clearly, Eq.9 can be given the actual form desired, including cases when the thermophysical properties varies between phases.

The system of coupled non-linear equations (4) and (9) are then solved over the domain of interest, subjected to the appropriate initial and boundary conditions for the phase and temperature fields. The S-L interface location can be determined a posteriori, simply by locating the points where the phase variable p crosses zero. In this respect, the PF model is particularly suited for multidimensional solidification problems, since curvature and anisotropic effects are implicitly taken into account⁹.

VALIDATION OF PHASE-FIELD SOLUTIONS

Benchmark quantitative tests were intensively made for the PF solutions^{4,5,8,10}, and they allow confidence in the numerical results for engineering applications. The numerical method to solve Eqs. 7 and 9 can be as simple as an iterated finite-difference discretization over a fixed uniform grid, or it's companion conservative control-volume scheme; those are detailed described elsewhere^{4,5,10}.

As an example, we show in Fig. 4 the results for water solidification ($K_l=5.64 \times 10^{-4} \text{ kJ/ms}^\circ\text{C}$, $K_s=2.24 \times 10^{-3} \text{ kJ/ms}^\circ\text{C}$, $c_l=4.2 \text{ kJ/kg}^\circ\text{C}$, $c_s=2.02 \text{ kJ/kg}^\circ\text{C}$, $\rho_l=\rho_s=960 \text{ kg/m}^3$, $L=333.4 \text{ kJ/kg}$), as compared to the analytical Newman solution¹. The domain length is taken $l = 2\text{cm}$, initially with uniform temperature $T_{hot}=10^\circ\text{C}$. Solidification takes place by imposing the boundary condition $T(0,t)=T_{cold}=-5^\circ\text{C}$ for $t>0$. In order to compare the numerical PF results with the semi-infinite slab similarity solution, we started the computation after growth of an initial layer of solid, at $x_0=0.1\text{cm}$, and maintain the temperature at the right end ($x = l$) at the values predicted by the Newman solution. The PF kinetic undercooling was given, in this benchmark run, the small value of $T^0=-0.002^\circ\text{C}$ (lower

values yield better emulation of the sharp classical interface problem, at the expense of increasing effort in computation time). The interfacial tension, for the sake of this comparison, is also a convenient numerical parameter, which in the case of a simple fixed-grid discretization should correspond to an interfacial characteristic length not smaller than the mesh interval – we choose $\xi=1.25\Delta x$. All computations were done by a 500 point mesh.

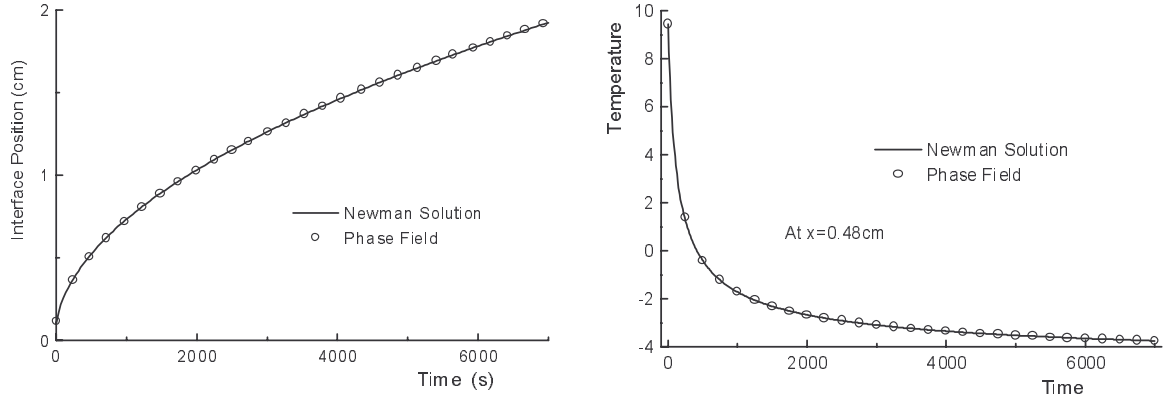


Fig. 4 – Interface progression in time and temperature history at $x=0.48\text{cm}$ for a semi-infinite slab solidification of water (no supercooling).

THE SUPERCOOLED TWO-PHASE STEFAN PROBLEM

A more stringent test, which is also better suited to the PF model, is the solidification from an initially supercooled melt ($T(x,0)=T_{\text{init}} < T_m$, and $T(0,t)=T_s < T_m$ for $t>0$). This gives rise to the so-called “two-phase supercooled Stephan problem”, and it is classically modeled by imposing an S-L interface at $T=T_m$, which advances through the melt by heat release from the latent heat source. In this case, heat transport is away from the interface in both directions (to the melt and to the solid), since the greatest temperature is at $x=\Gamma(t)$. It is well-known that it is not possible, in more than one dimension, to maintain a flat stable interface in that situation¹¹. In one-dimensional approximations (slab solidification), there is also a similarity analytical solution for semi-infinite domains², which we transcribe here for convenience:

$$\Gamma(t) = 2\lambda\sqrt{\alpha_s t}$$

$$T_{\text{solid}}(x,t) = T_s + (T_m - T_s) \frac{\text{erf}\left(\frac{x}{2\sqrt{\alpha_s t}}\right)}{\text{erf}(\lambda)} \quad , \text{ for } 0 \leq x \leq \Gamma(t) \quad (\text{Eq. 10a})$$

$$T_{\text{liquid}}(x, t) = T_{\text{init}} + (T_m - T_{\text{init}}) \frac{\text{erfc}(\frac{x}{2\sqrt{\alpha_l t}})}{\text{erfc}(v\lambda)} , \text{ for } \Gamma(t) \leq x \leq \infty \quad (10b)$$

, where λ is a root of the transcendental equation

$$\frac{St_s}{\lambda \sqrt{\pi} e^{\lambda^2} \text{erf}(\lambda)} + \frac{St_{\text{init}}}{(v\lambda) \sqrt{\pi} e^{(v\lambda)^2} \text{erfc}(v\lambda)} = 1 \quad (10c)$$

and the Stefan numbers

$$St_s = \frac{c_s (T_m - T_s)}{L} \quad St_{\text{init}} = \frac{c_l (T_m - T_{\text{init}})}{L} \quad (10d)$$

α_l, α_s are the heat diffusivities in the liquid and solid phases ($= K/\rho c$), with $v = \sqrt{\alpha_s/\alpha_l}$.

$\text{erf}(x)$ is the error function and $\text{erfc}(x) = 1 - \text{erf}(x)$.

The above classical solution is valid whenever the liquid is not hypercooled, that is to say, if the latent heat release is enough to raise the temperature of the supercooled liquid from T_{init} to T_m (which implies the condition $0 < St_{\text{init}} < 1$).

Clearly, supercooled solidification poses a major difficulty for the traditional numerical methods, since there is not a well-defined enthalpy-temperature relationship in this case. The front-tracking methods would have to rely in the condition that a liquid element would undergo solidification only when its temperature is raised to T_m and is about to be traversed by the solid-liquid interface – a somewhat clumsy condition to follow in the presence of more general, or time-dependent, boundary conditions or sources of heat.

PHASE-FIELD SOLUTIONS TO THE SUPERCOOLED STEFAN PROBLEM

The PF model applies naturally to supercooled solidification. As before, we consider a 5cm slab of water initially at -10°C but still liquid, impose the fixed temperature -20°C at the wall $x=0$, and started solidification at $t=0$.

It should be noted that the nucleation process at $x=0$, which started the solidification process at $t=0$, is not an issue here. In fact, nucleation cannot be taken into account by a mean-field model (such the Phase-Field free-energy minimization, based on the Landau expansion to the second order, Eq.3). Being a fluctuation process, nucleation could be simulated within the PF model by introducing noise in the phase evolution equation.

The results of the PF calculations were compared to the similarity solutions after an initial layer of solid was already grown up to $x_0=0.5\text{cm}$. The boundary temperature at $x=l$ was kept time-dependent, equal to $T_{\text{liquid}}(l,t)$ (Eq. 10b).

The results are shown in Figs. 5-7, along with the numerical PF results for a supercooled solidification inside the finite domain $[0,l]$ when $T(l,t)$ is kept constant at -10°C .

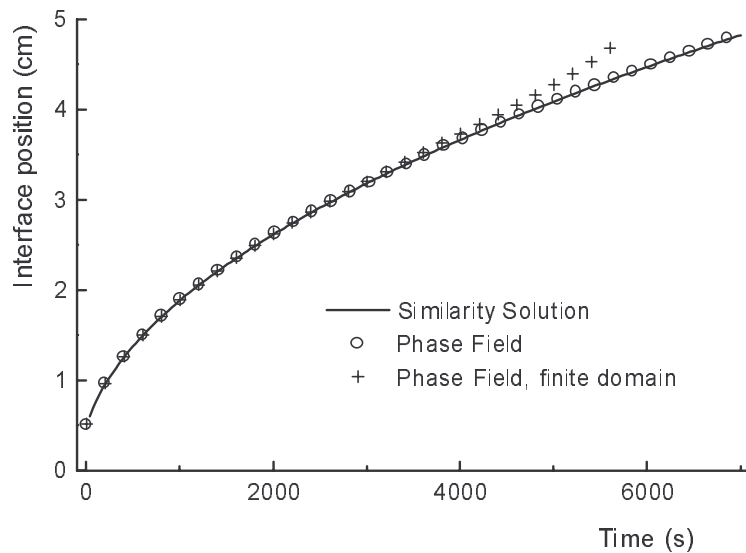


Fig. 5 – Interface progression in time, supercooled slab of water solidification.

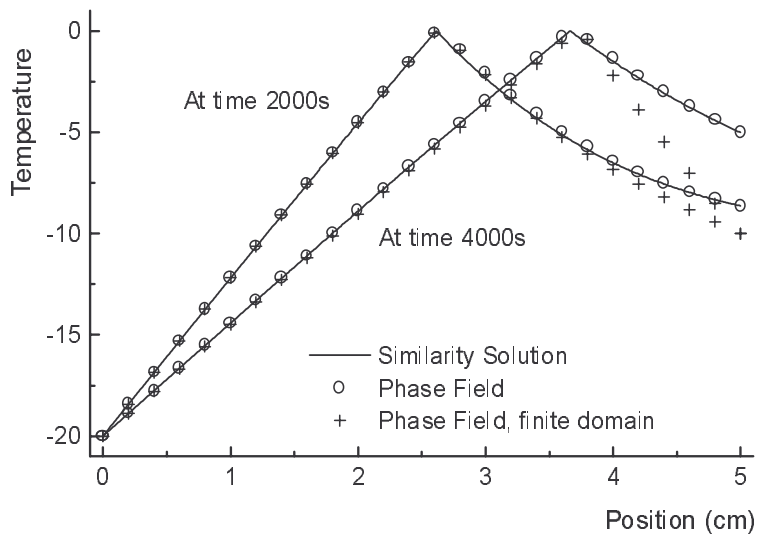


Fig. 6 – Temperature fields at times 2000s and 4000s.

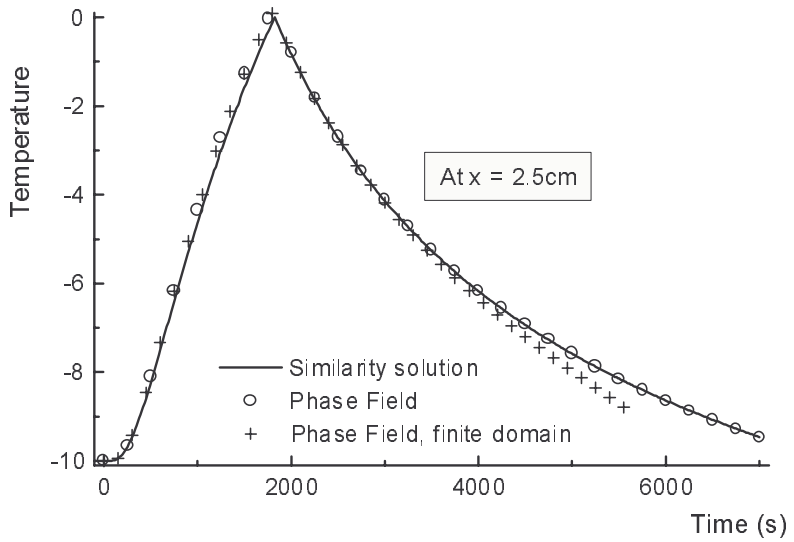


Fig. 7 – Temperature history at the position 2,5cm.

At this level of mesh refining, the PF numerical results differ from the analytical solution by less than 5% (relative error). We therefore can be confident that the numerical solutions for the finite domain case are reliable enough for engineering applications.

All runs were made with a 500 point mesh. No code optimization were done in the numerical implementation, which was a simple iterated totally-implicit control-volume discretization, with linearized source terms¹⁰. The convergence of the numerical scheme was carefully tested and reported elsewhere^{4,10}. A typical run takes an hour of CPU time in a 250MHz Pentium MMX PC, running code generated by the GNU-C compiler under DOS/Windows 95.

It is worth noting that numerical PF implementations require a somewhat refined mesh around the interface (where ∇p is high), if results are to be referred to the (still in wider acceptance) classical sharp interface models. Fig.8 shows the predicted interface temperature for distinct mesh sizes, where it can be seen that the S-L temperature stabilizes to $T^0 = -0.002$ only for higher mesh resolutions.

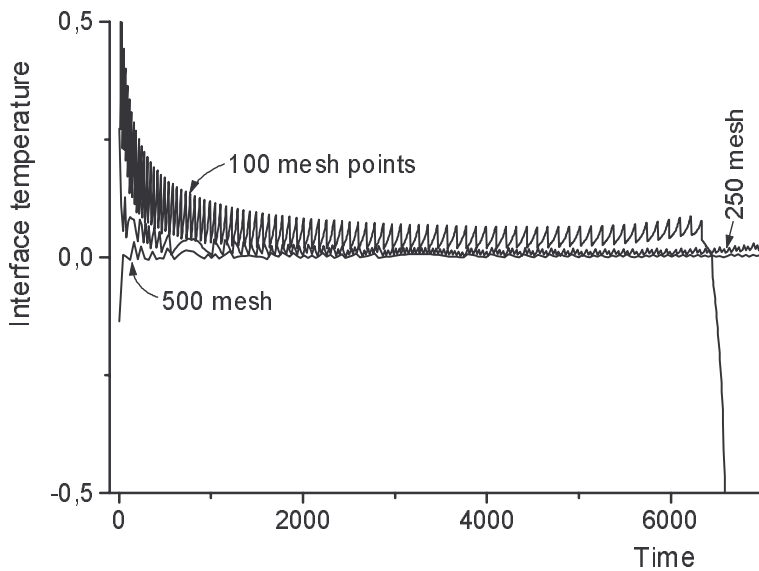


Fig. 8 – Temperature at the S-L interface as obtained by the PF calculations for increasing mesh sizes.

CONCLUSIONS AND COMMENTS

The PF model, while providing a better physical description of solidification dynamics, also allows for a numerical implementation avoiding the explicit tracking of the solid-liquid interface. The non-linear evolution equation for the phase parameter can be coupled to any other transport or constitutive law for the thermodynamic quantities involved in the solidification process. Numerically, the PF technique has been shown to be as accurate as the more traditional sharp-interface descriptions, which frequently are based in *ad-hoc* assumptions about the interface dynamics.

The parameters that govern the scales of the phase variable, namely, the kinetic coefficient and the surface tension, which in this work were taken merely as convenient numerical constants, can be matched to the actual medium physical values¹², thus allowing for realistic simulations of generalized solidification processes (involving dendrite growth and facets, for instance).

Current limitations of the phase-field descriptions are the artificial cutoff at short wavelengths due to the numerical discretization and the high computational effort required for two and three-dimensional calculations. There are also some controversy about the thermodynamic consistency of the PF functional, particularly when coupled to non-conservative transport, viscous convection, or other types of phase transitions. But all of those issues are likely to be amenable to better theoretical and numerical techniques and are topics of active research.

ACKNOWLEDGEMENTS

The Author would like to acknowledge research grants from the PEPCI/USF program (Programa de Estímulo à Pesquisa Científica – Universidade São Francisco) and FAPESP (Fundação de Amparo à Pesquisa do Estado de São Paulo).

REFERENCES

1. CARSLAW, H.S. and JAEGER, J.S. "Conduction of Heat in Solids", 2a. Ed, Clarendon Press, Oxford, 1959.
2. ALEXIADES, V. and SOLOMON, A.D. "Mathematical Modeling of Melting and Freezing Processes", Hemisphere, Washington, 1993.
3. CAGINALP, G. and SOCOLOVSKY, E.A. "Computation of Sharp Phase Boundaries by Spreading: The Planar and Spherical Symmetric Cases", *J.Comp.Phys.* **95**, pp.85-100, 1991.
4. FABBRI, M. and VOLLE, V.R. "The Phase-Filed Method in the Sharp-Interface Limit: A Comparison Between Model Potentials", *J.Comp.Phys.* **130**, pp.256-265, 1997.
5. FABBRI, M. "The Phase-Field Method in Engineering: Behavior Under Various Solidification Regimes", *Proceedings of the 5th Thermal Sciences Brazilian Meeting*, São Paulo, SP, Brazil, pp. 329-333, Dec. 1994.
6. ALLEN, S.M. and CAHN, J.W. "A Microscopic Theory for Antiphase Boundary Motion and its Application to Antiphase Domain Coarsening", *Acta Metall.* **27**, pp.1085-1095, 1979.
7. KOBAYASHI, R. "Modeling and Numerical Simulations of Dendritic Crystal Growth", *Physica D* **63**, pp.410-423, 1993.
8. FAZENDA, A.L.; TRAVELHO, J.S. and FABBRI, M. "Modeling Kinetic Undercooling Through Phase-Field Equations With Non-Linear Dynamics", *Proceedings of the 6th Thermal Sciences Brazilian Meeting*, Florianópolis, SC, Brazil, pp. 953-956, Nov. 1996.
9. WARREN, J.A. "How Does a Metal Freeze? A Phase-Field Model of Alloy Solidification", *IEEE Comp.Sci.Eng.* **2**(2), pp.39-49, 1995.
10. FABBRI, M. and VOLLE, V.R. "Numerical Solution of Plane-Front Solidification With Kinetic Undercooling", *Num. Heat Transf.* **27**(4), pp.467-486, 1995.
11. KURZ, W. and FISHER, D.J. "Fundamentals of Solidification", Trans-Tech Publications, Switzerland, 1992.

12. CAGINALP, G. and XIE, W. "Phase-Field and Sharp-Interface Alloy Models", *Phys.Rev. E* **48**(3), pp.1897-1909, 1993.